

Electronic Supplementary Information for

Insertion chemistry of iron(II) boryl complexes

Ana L. Narro, Hadi D. Arman and Zachary J. Tonzetich*

Department of Chemistry, University of Texas at San Antonio (UTSA), San Antonio, TX 78249

zachary.tonzetich@utsa.edu

CONTENTS	Pages
Figure S1. ^1H NMR spectrum of $[\text{Fe}(\text{Bpin})(^{\text{Cy}}\text{PNP})]$ (3a) generated from 1 · py in benzene- d_6 .	S2
Figure S2. ^1H NMR spectrum of $[\text{Fe}(\text{Bpin})(^{\text{Cy}}\text{PNP})]$ (3a) generated from 2 in toluene- d_8	S3
Figure S3. ^1H NMR spectrum of $[\text{Fe}(\text{Bcat})(^{\text{Cy}}\text{PNP})]$ (3b) in benzene- d_6 .	S4
Figure S4. ^1H NMR spectrum of putative $[\text{Fe}(\text{Bcat})(\text{CO})_2(^{\text{Cy}}\text{PNP})]$ (3b · CO) in benzene- d_6 .	S5
Figure S5. ^1H NMR spectrum of the reaction of 3b with 2,2'-bipyridine in benzene- d_6 .	S6
Figure S6. ^1H NMR spectrum of $[\text{Fe}(\text{CO})_2(\text{OPh})(^{\text{Cy}}\text{PNP})]$ (1 · CO) in benzene- d_6 .	S7
Figure S7. ^1H NMR spectrum of $[\text{Fe}(\text{bipy})(\text{OPh})(^{\text{Cy}}\text{PNP})]$ (1 · bipy) in benzene- d_6 .	S8
Figure S8. ^1H NMR spectrum of $[\text{Fe}(\text{C}\{\text{Me}\}\text{C}\{\text{Me}\}\text{Bpin})(^{\text{Cy}}\text{PNP})]$ (4a) in benzene- d_6 .	S9
Figure S9. ^1H NMR spectrum of $[\text{Fe}(\text{C}\{\text{Me}\}\text{C}\{\text{Me}\}\text{Bcat})(^{\text{Cy}}\text{PNP})]$ (4b) in benzene- d_6 .	S10
Figure S10. ^1H NMR spectrum of $[\text{Fe}(\text{C}\{\text{Ph}\}\text{C}\{\text{H}\}\text{Bpin})(^{\text{Cy}}\text{PNP})]$ (5a) in benzene- d_6 .	S11
Figure S11. ^1H NMR spectrum of $[\text{Fe}(\text{C}\{\text{Ph}\}\text{C}\{\text{H}\}\text{Bcat})(^{\text{Cy}}\text{PNP})]$ (5b) in toluene- d_8 .	S12
Figure S12. ^1H NMR spectrum of $[\text{Fe}(\text{C}\{\text{Ph}\}\text{C}\{\text{Me}\}\text{Bpin})(^{\text{Cy}}\text{PNP})]$ (6a) in toluene- d_8 .	S13
Figure S13. ^1H NMR spectrum of $[\text{Fe}(\text{C}\{\text{Ph}\}\text{C}\{\text{CCPh}\}\text{Bpin})(^{\text{Cy}}\text{PNP})]$ (7a) in benzene- d_6 .	S14
Figure S14. ^1H NMR spectrum of $[\text{Fe}(\text{C}\{\text{Ad}\}\text{NBpin})(^{\text{Cy}}\text{PNP})]$ (8) in benzene- d_6 .	S15
Figure S15. ^{19}F NMR spectrum of the reaction of 3a and 4-fluorostyrene in benzene- d_6 .	S16
Figure S16. Thermal ellipsoid drawing (50%) of the solid-state structure of $\text{PhO}(\text{py})\text{Bcat}$.	S17
Figure S17. Thermal ellipsoid drawing (50%) of the solid-state structure of 1 · CO .	S18
Figure S18. Thermal ellipsoid drawing (50%) of the solid-state structure of 1 · bipy .	S19
Figure S19. Thermal ellipsoid drawing (50%) of the solid-state structure of 5b .	S20
Figure S20. Thermal ellipsoid drawing (50%) of the solid-state structure of 6a .	S21
Figure S21. Thermal ellipsoid drawing (50%) of the solid-state structure of 7a .	S22

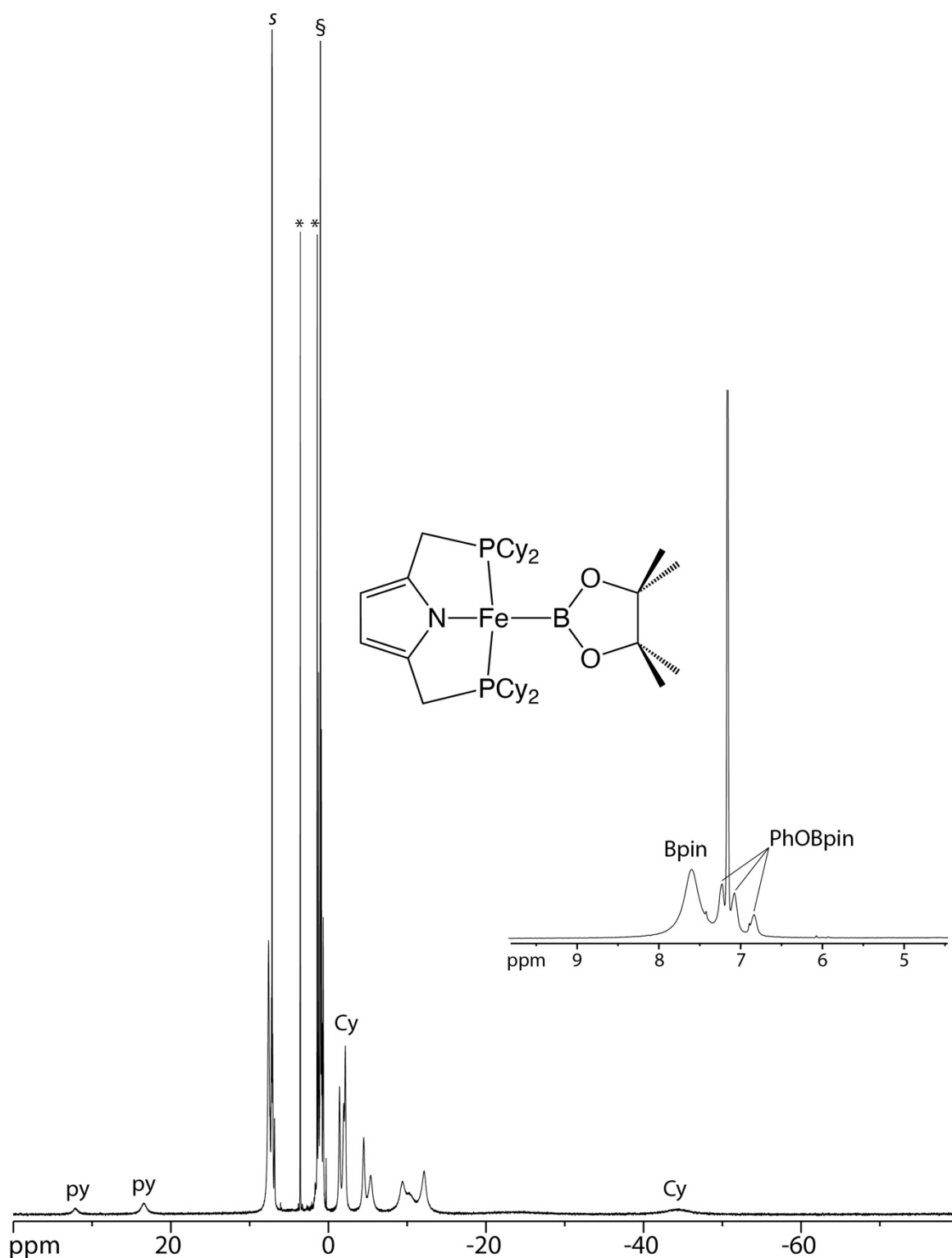


Figure S1. 300 MHz ¹H NMR spectrum of [Fe(Bpin)(^{Cy}PNP)] (**3a**) in benzene-*d*₆(*s*) generated from the reaction of **1·py** and B₂pin₂. Inset displays an expansion of the region from 4 to 10 ppm showing peaks for the expected byproduct, PhOBpin. Asterisks denote resonances for thf used in the preparation of **1·py**. The resonance for excess B₂pin₂ and PhOBpin is marked with §.

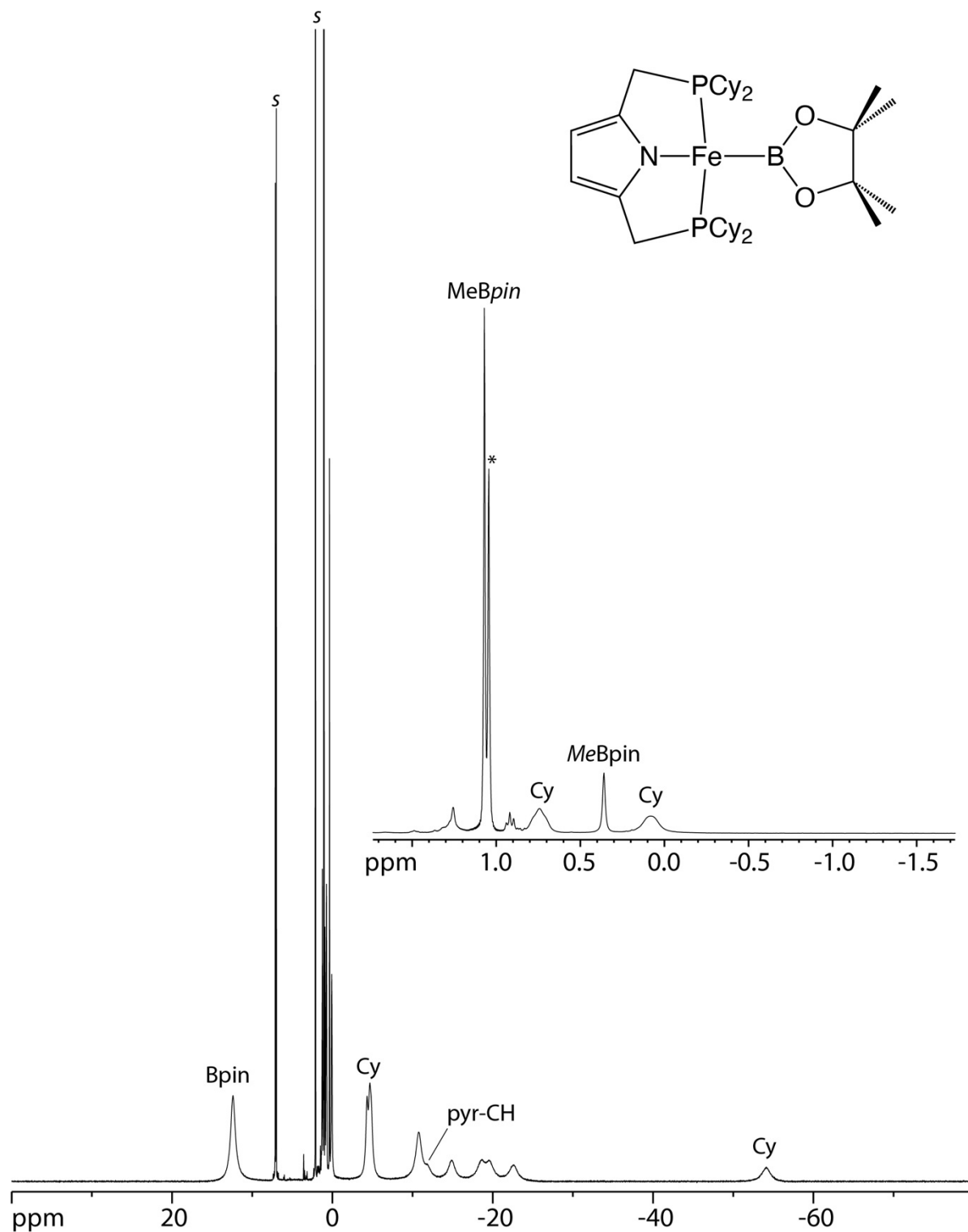


Figure S2. 300 MHz ^1H NMR spectrum of $[\text{Fe}(\text{Bpin})(\text{CyPNP})]$ (**3a**) in $\text{toluene-}d_8(s)$ generated from the reaction of **2** and B_2pin_2 . Inset displays an expansion of the region from -2 to 2 ppm showing peaks for the expected byproduct, MeBpin. Asterisk denotes the resonance for excess B_2pin_2 .

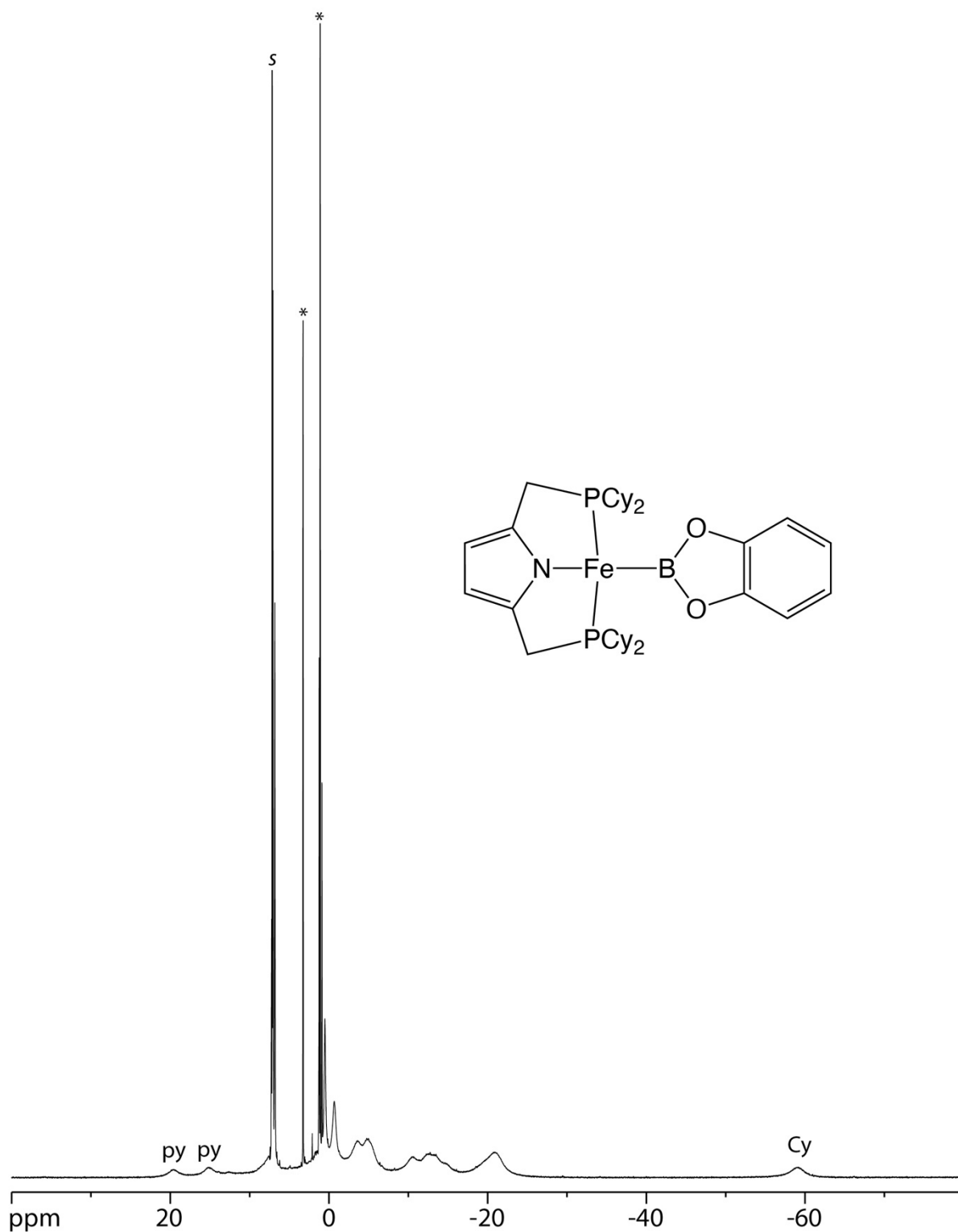


Figure S3. 300 MHz ^1H NMR spectrum of $[\text{Fe}(\text{Bcat})(\text{CyPNP})]$ (**3b**) in benzene- d_6 (s) generated from the reaction of **1·py** and B_2cat_2 . Asterisks denotes resonances for Et_2O used in purification of **1·py**.

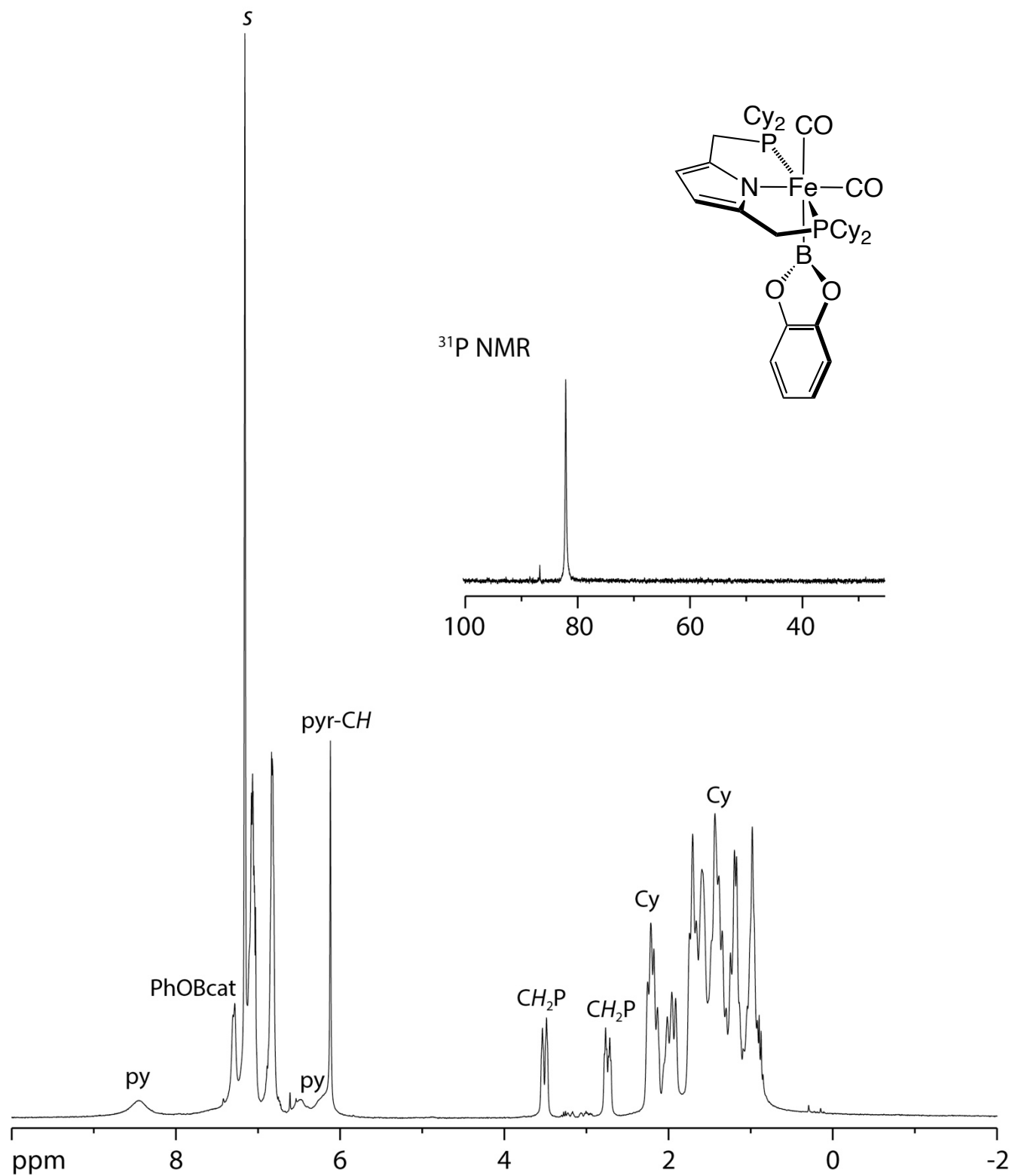


Figure S4. 300 MHz ^1H NMR spectrum of putative $[\text{Fe}(\text{Bcat})(\text{CO})_2(\text{CyPNP})]$ (**3b**·CO) in benzene- d_6 (s) generated from the reaction of **1**·py and B_2cat_2 followed by introduction of $\text{CO}(\text{g})$.

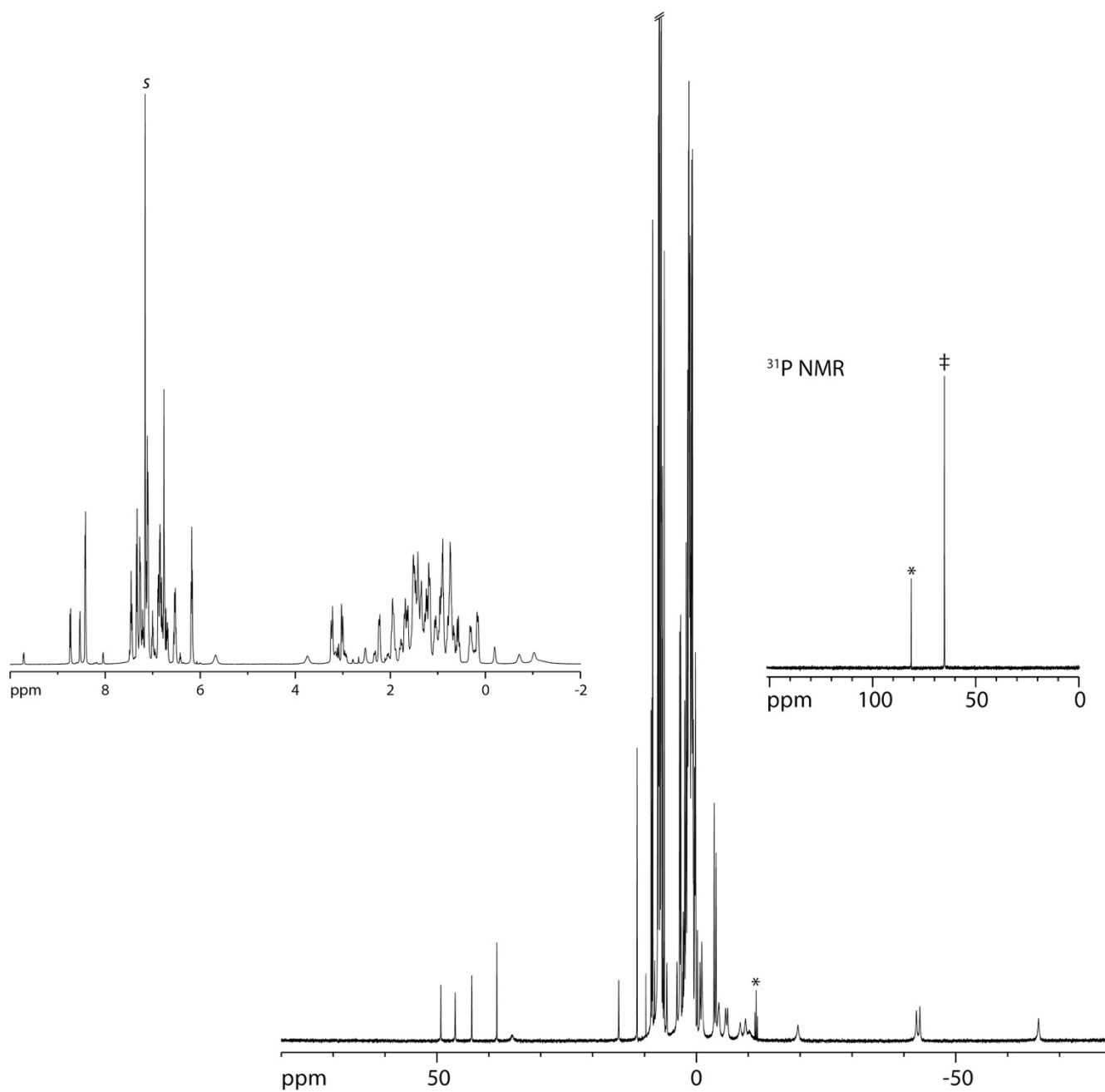


Figure S5. 300 MHz ^1H NMR spectrum of the reaction of in situ-generated $[\text{Fe}(\text{Bcat})(\text{CyPNP})]$ (**3b**) with 2,2'-bipyridine in benzene- $d_6(s)$. Left inset displays expansion of the diamagnetic region. Asterisks denote resonances for $[\text{FeH}(\text{bipy})(\text{CyPNP})]$. ^{31}P NMR resonance for putative **3b**·**bipy** is marked with ‡.

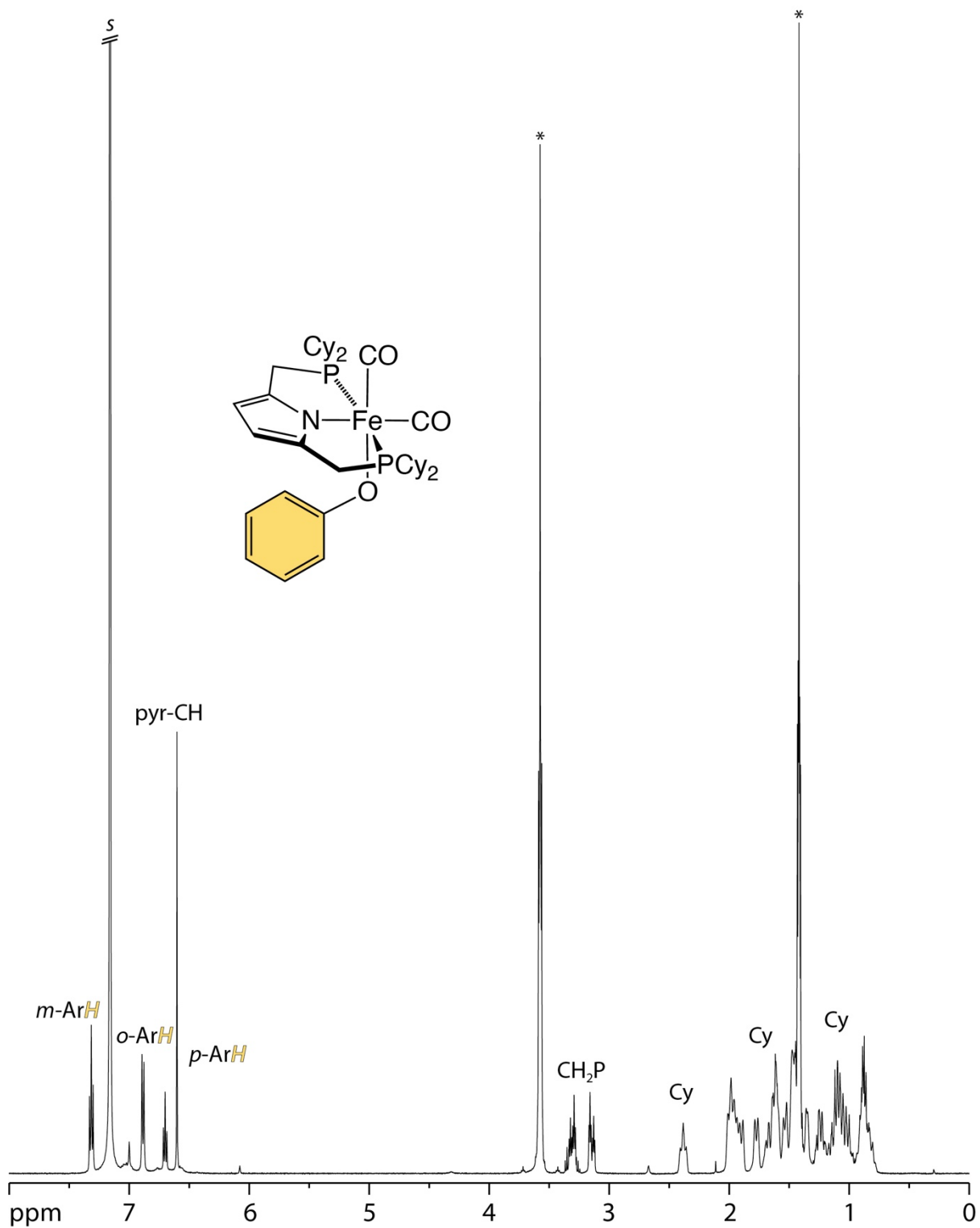


Figure S6. 500 MHz ^1H NMR spectrum of $[\text{Fe}(\text{CO})_2(\text{OPh})(\text{CyPNP})]$ (**1-CO**) in benzene- d_6 (s). Asterisks denotes resonances for thf used in preparation of **1-py**.

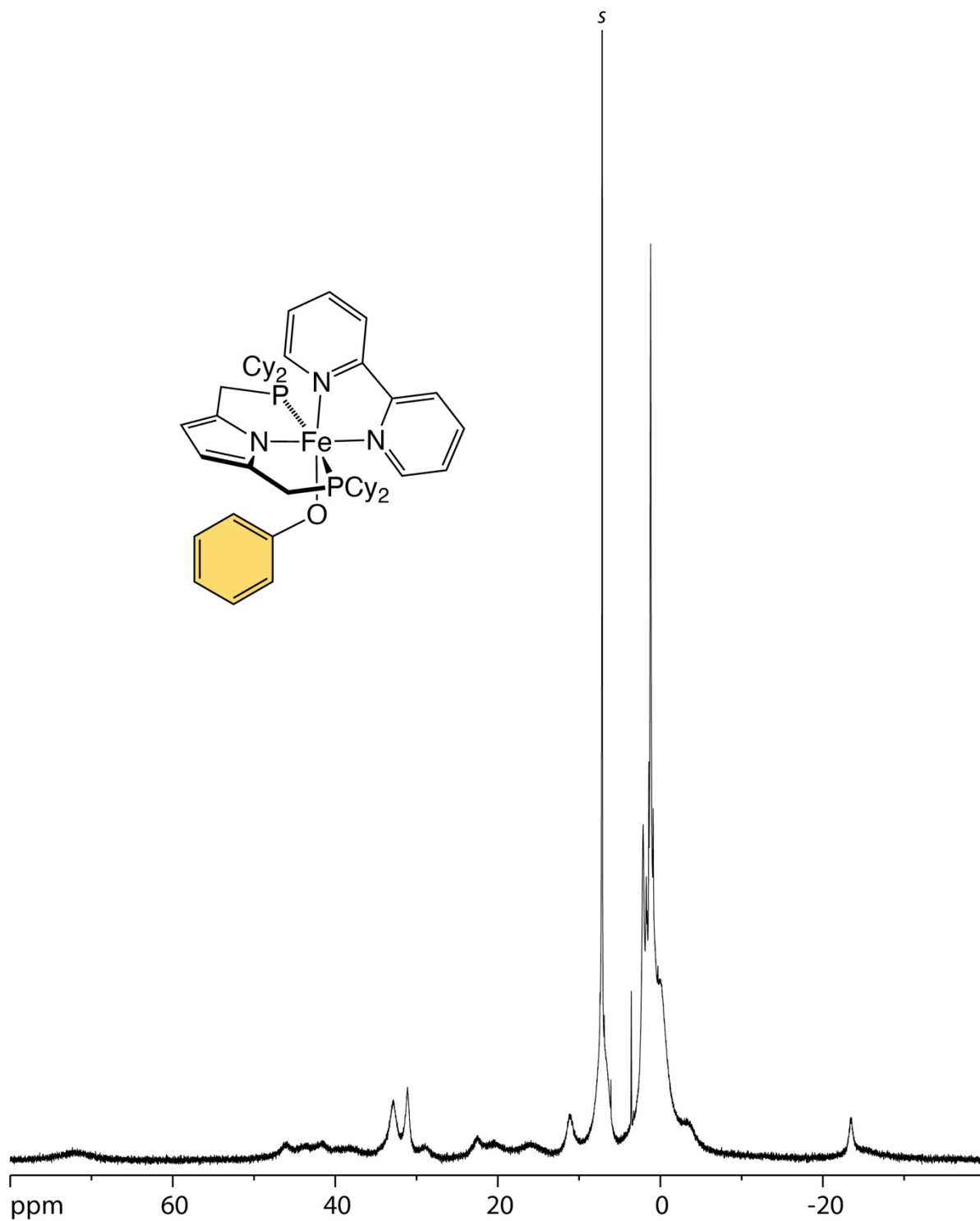


Figure S7. 300 MHz ¹H NMR spectrum of [Fe(bipy)(OPh)(^{Cy}PNP)] (**1·bipy**) in benzene-*d*₆(*s*).

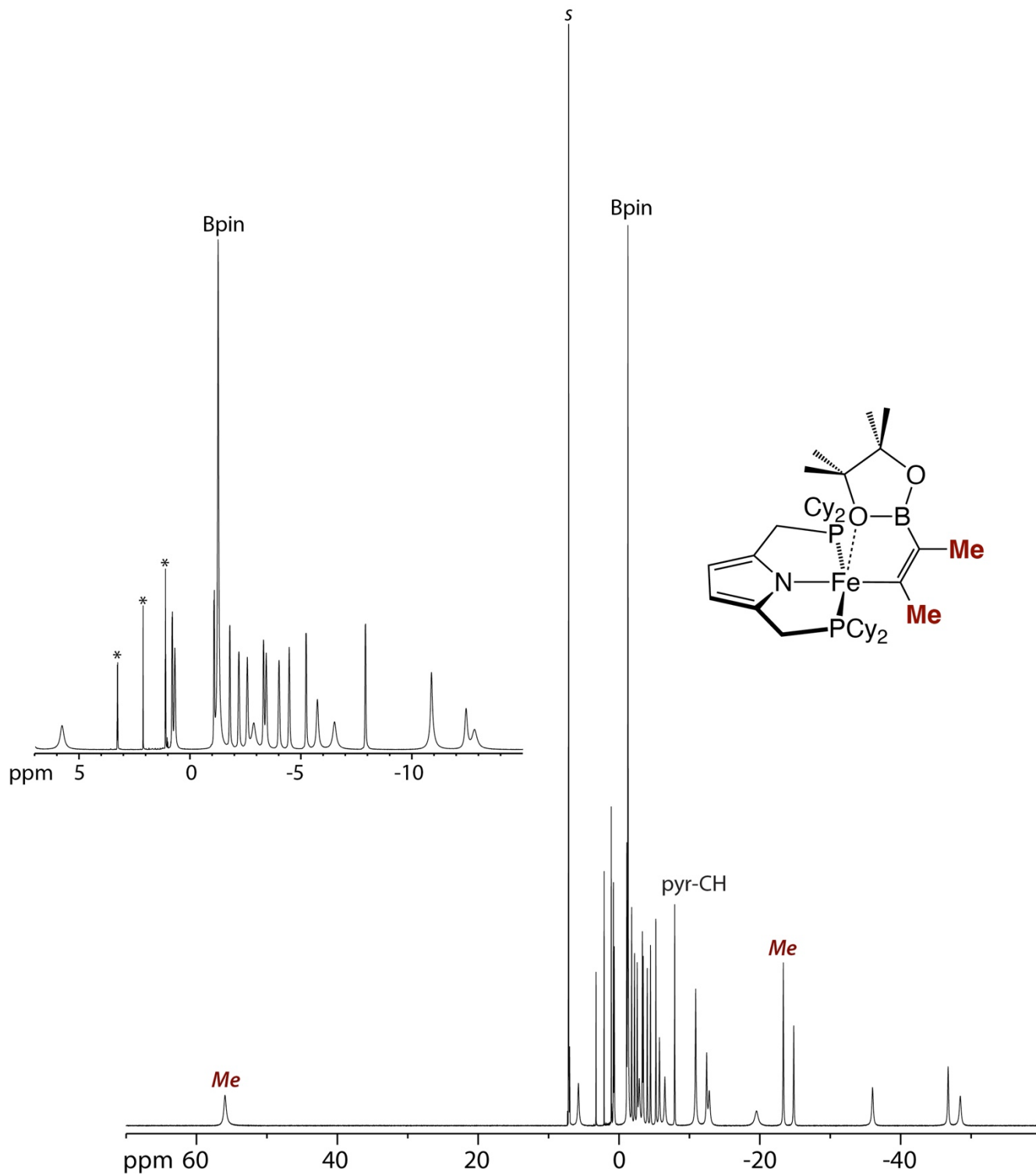


Figure S8. 300 MHz ^1H NMR spectrum of $[\text{Fe}(\text{C}\{\text{Me}\}\text{C}\{\text{Me}\}\text{Bpin})(\text{CyPNP})]$ (**4a**) in benzene- d_6 (s). Inset displays an expansion of the region from -15 to 7 ppm. Asterisks denote resonances for toluene and ether used in purification.

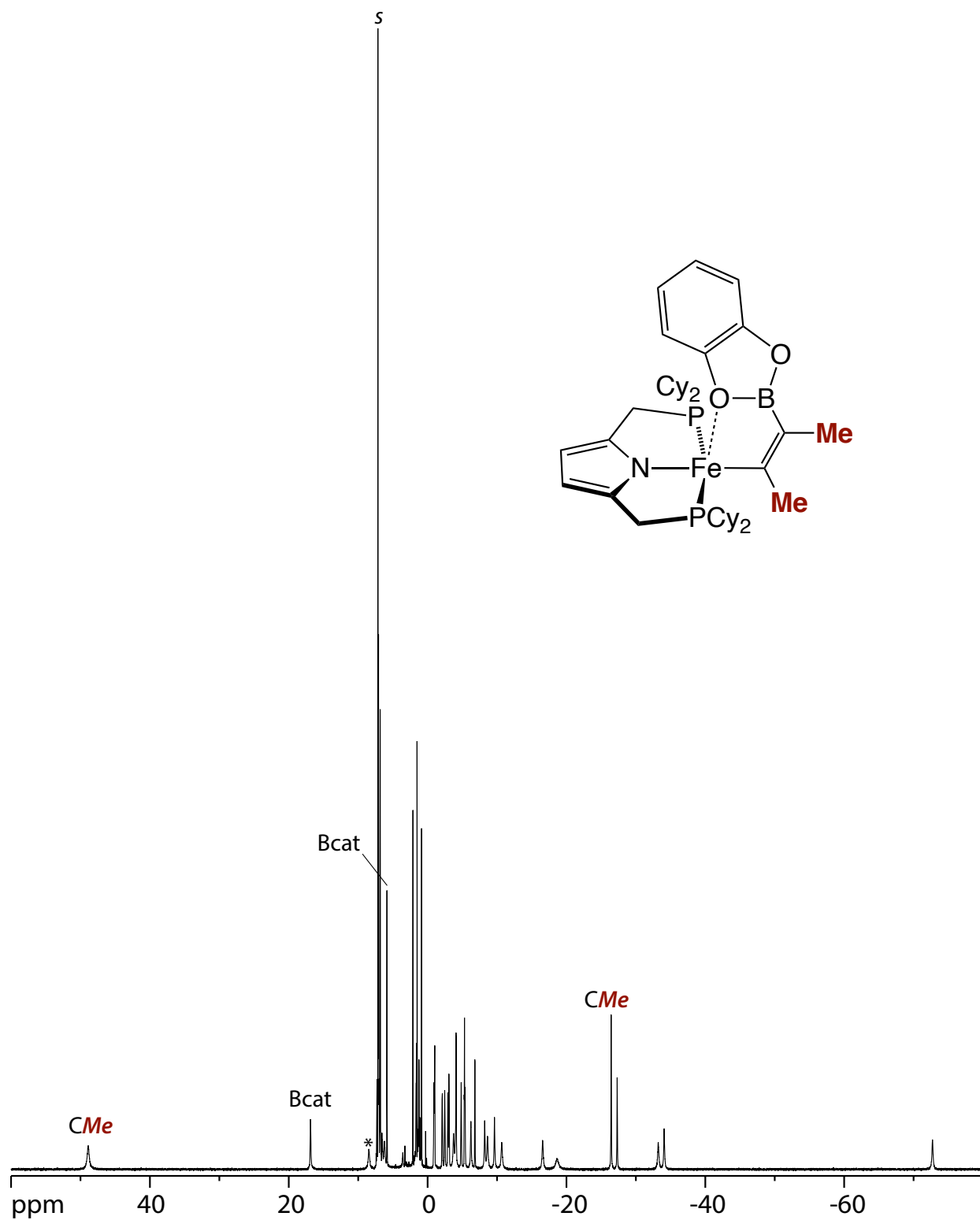


Figure S9. 300 MHz ^1H NMR spectrum of $[\text{Fe}(\text{C}\{\text{Me}\}\text{C}\{\text{Me}\}\text{Bcat})(\text{CyPNP})]$ (**4b**) in benzene- d_6 (s). Asterisks denote a resonance from the pyridine byproduct, PhOBcat.

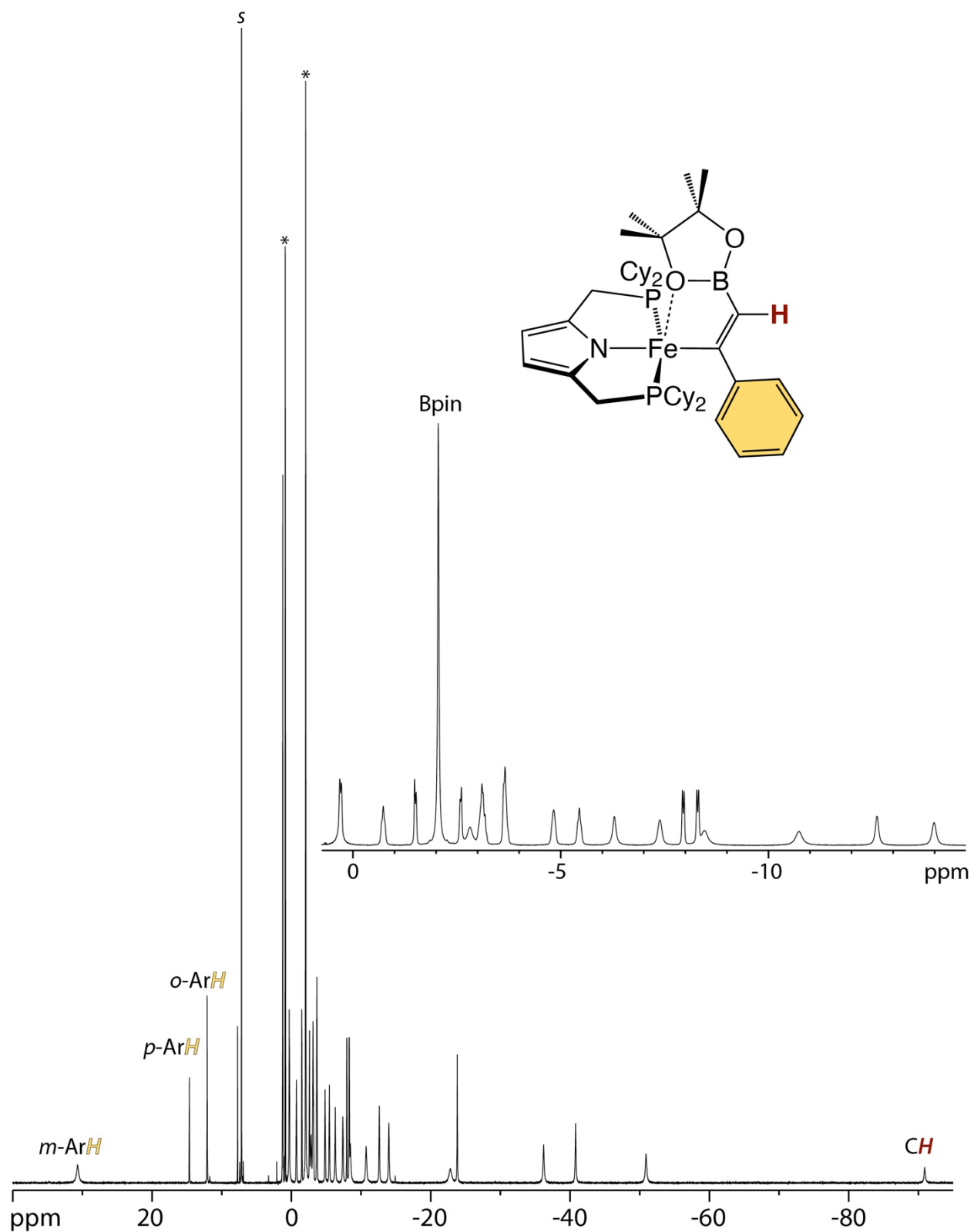


Figure S10. 300 MHz ^1H NMR spectrum of $[\text{Fe}(\text{C}(\text{Ph})\text{C}(\text{H})\text{Bpin})(\text{CyPNP})]$ (**5a**) in $\text{benzene-}d_6(s)$. Inset displays an expansion of the region from -15 to 1 ppm. Asterisks denote resonances for diethyl ether from purification.

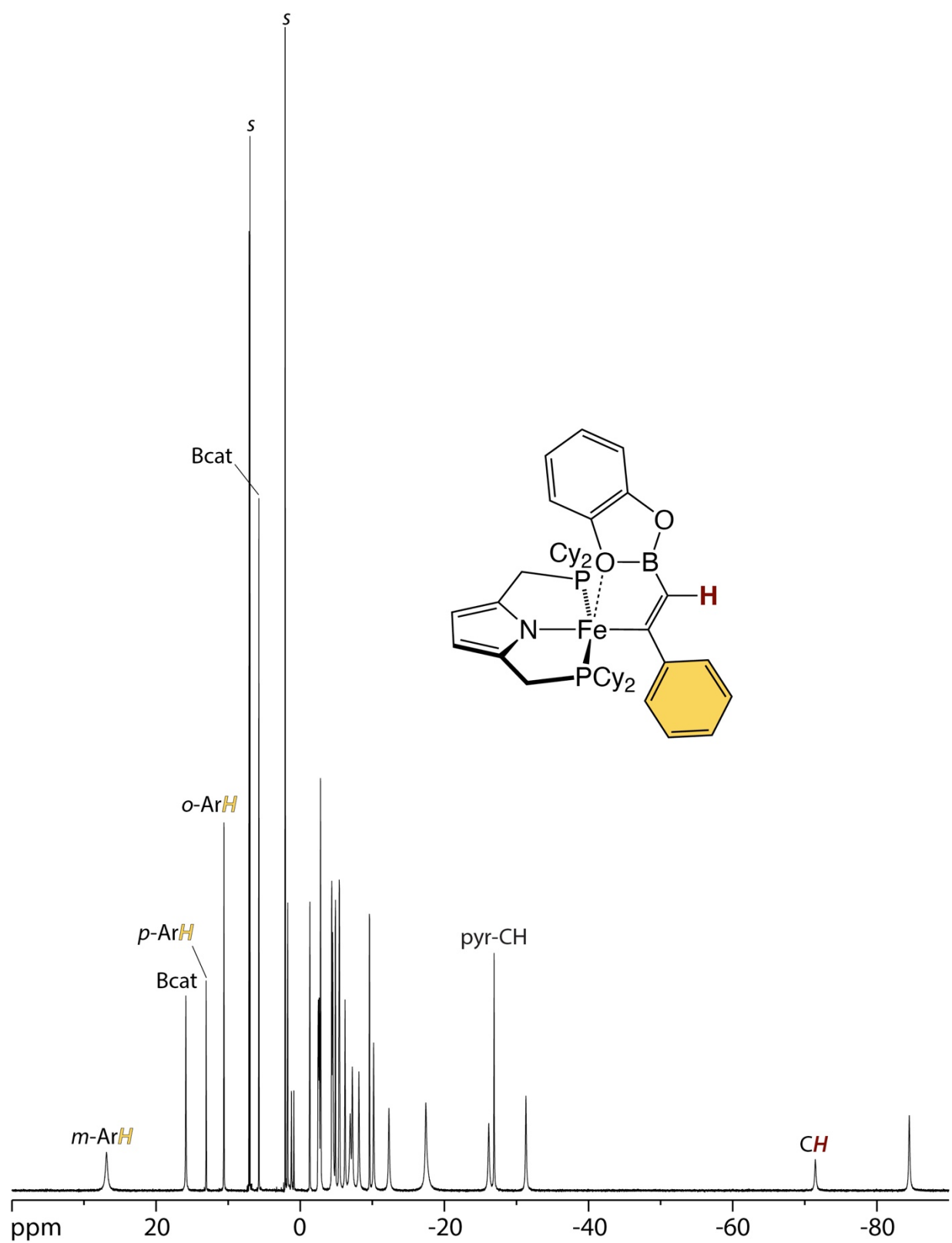


Figure S11. 300 MHz ¹H NMR spectrum of [Fe(C{Ph}C{H}Bcat)(^{Cy}PNP)] (**5b**) in toluene-*d*₈(*s*).

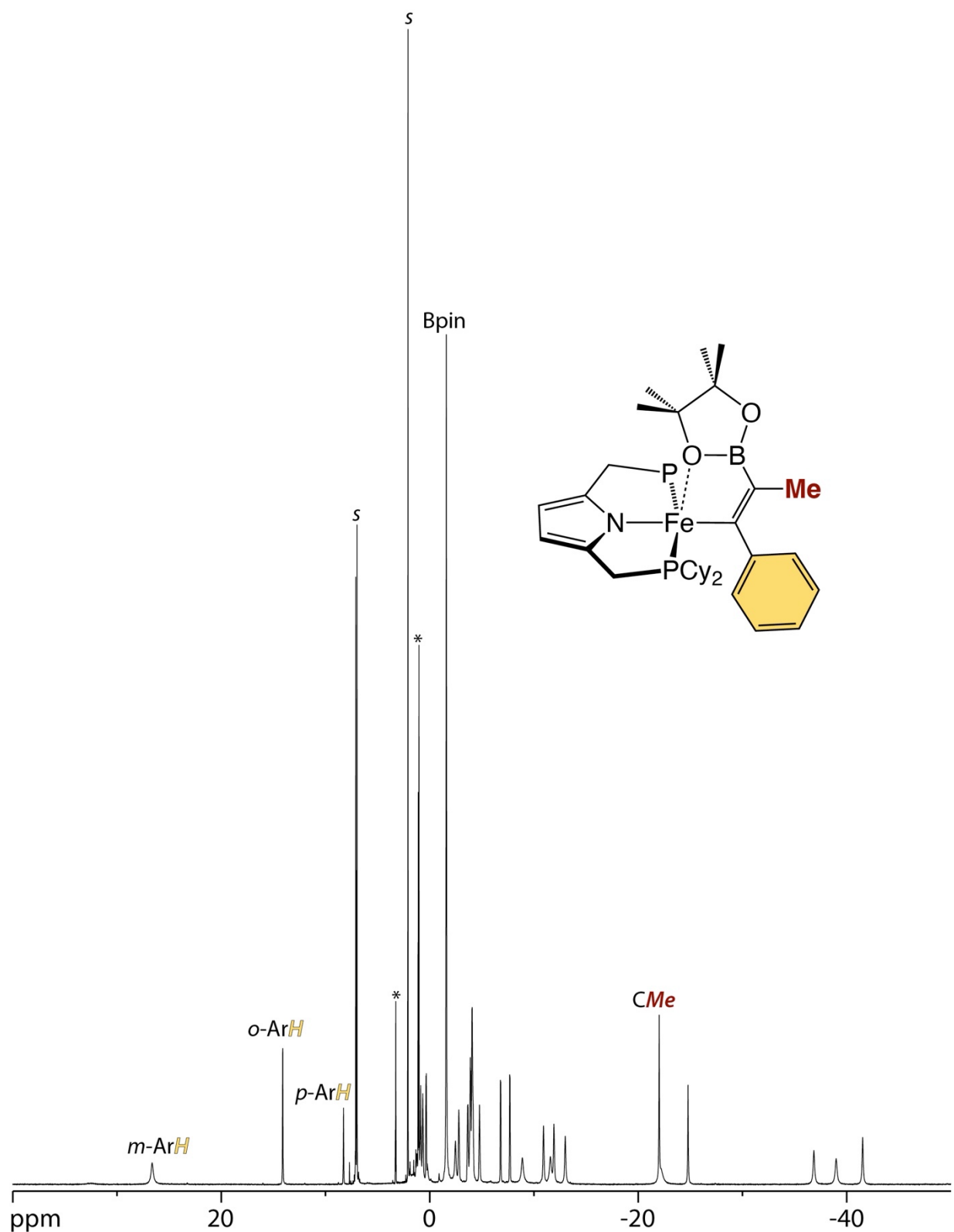


Figure S12. 300 MHz ¹H NMR spectrum of [Fe(C{Ph}C{Me}Bpin)(^{Cy}PNP)] (**6a**) in toluene-*d*₈(*s*). Asterisks denote resonances for diethyl ether from purification.

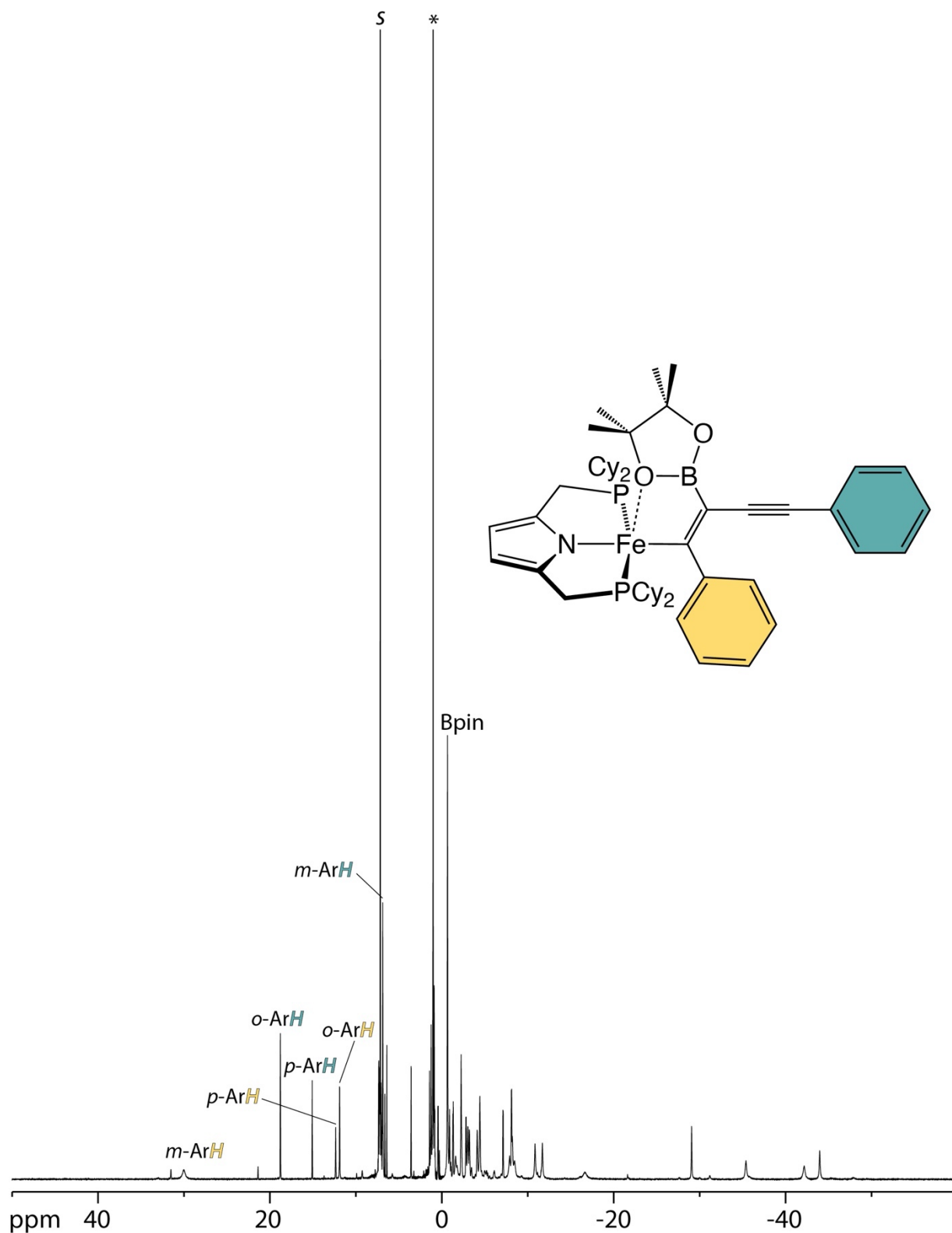


Figure S13. 300 MHz ^1H NMR spectrum of $[\text{Fe}(\text{C}(\text{Ph})\text{C}(\text{CPh})\text{Bpin})(\text{CyPNP})]$ (**7a**) in benzene- d_6 (s). Asterisk denotes resonances for residual B_2pin_2 used in preparation of **3a**.

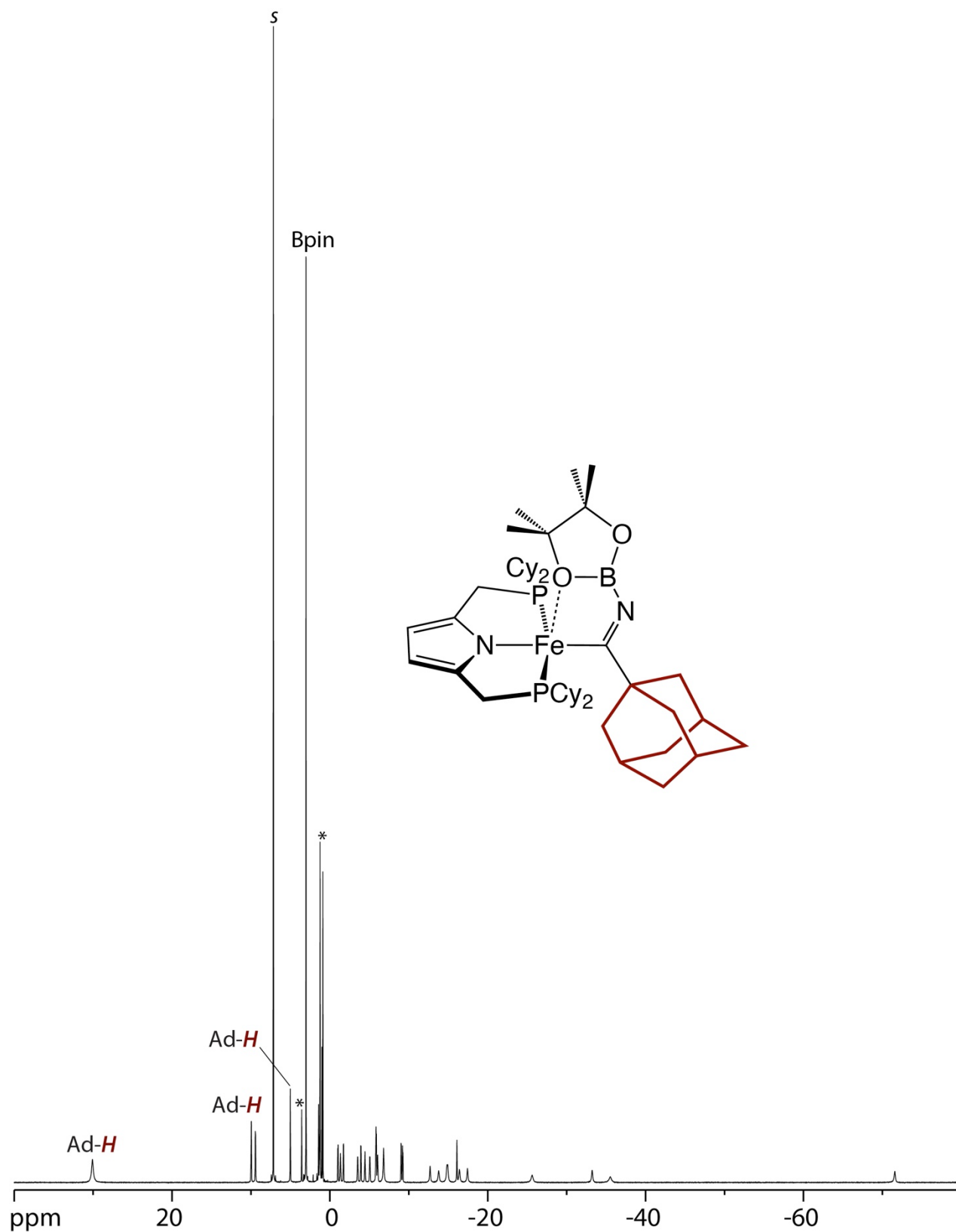


Figure S14. 300 MHz ^1H NMR spectrum of $[\text{Fe}(\text{C}\{\text{Ad}\}\text{NBpin})(\text{Cy}_2\text{PNP})]$ (**8**) in benzene- d_6 (s).

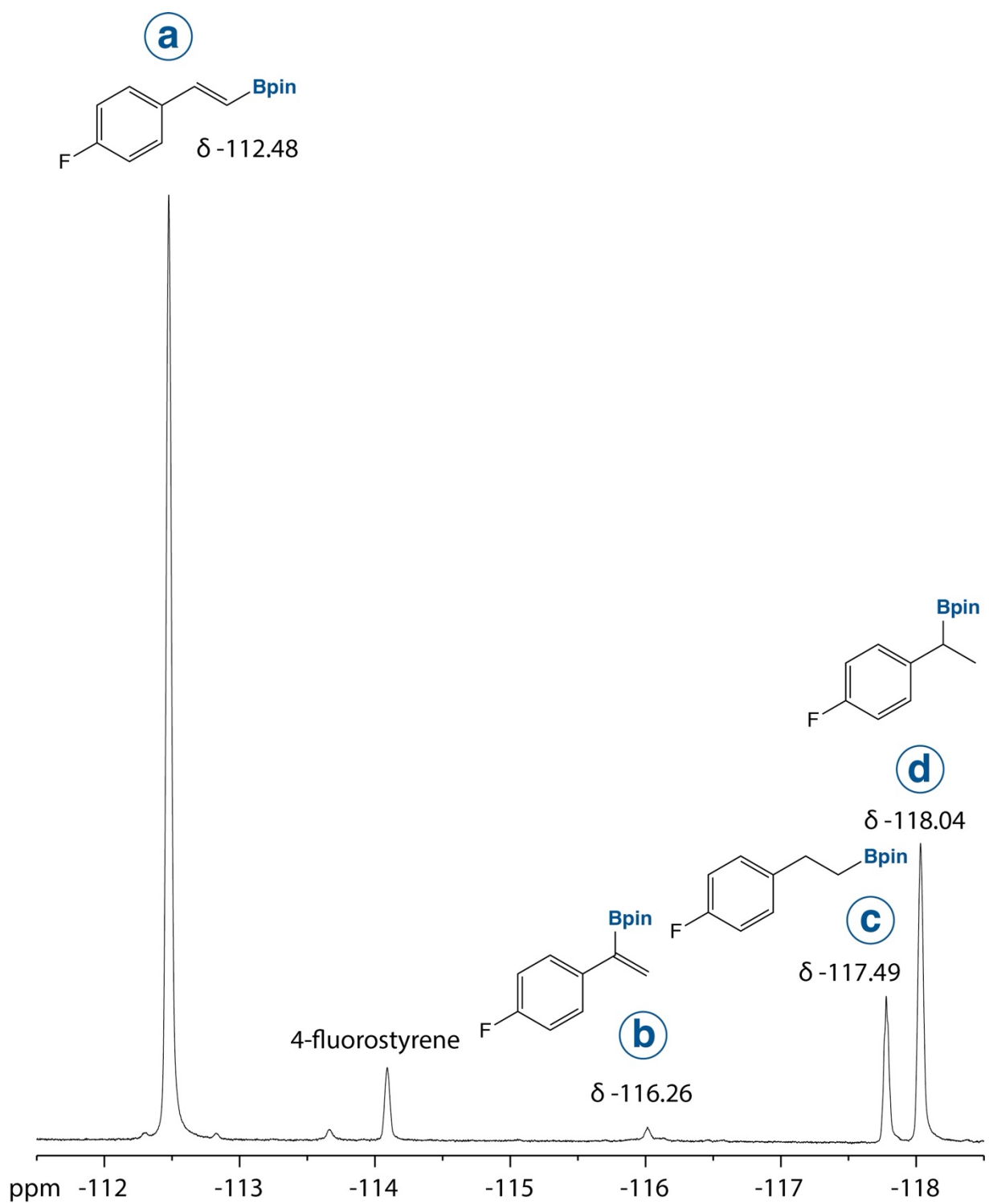


Figure S15. Selected region of the ^{19}F NMR spectrum of the reaction of **3a** and 4-fluorostyrene in benzene- d_6 (s) showing formation of borylated products. Product assignments (a – d) correspond to those in Scheme 4 of the main text.

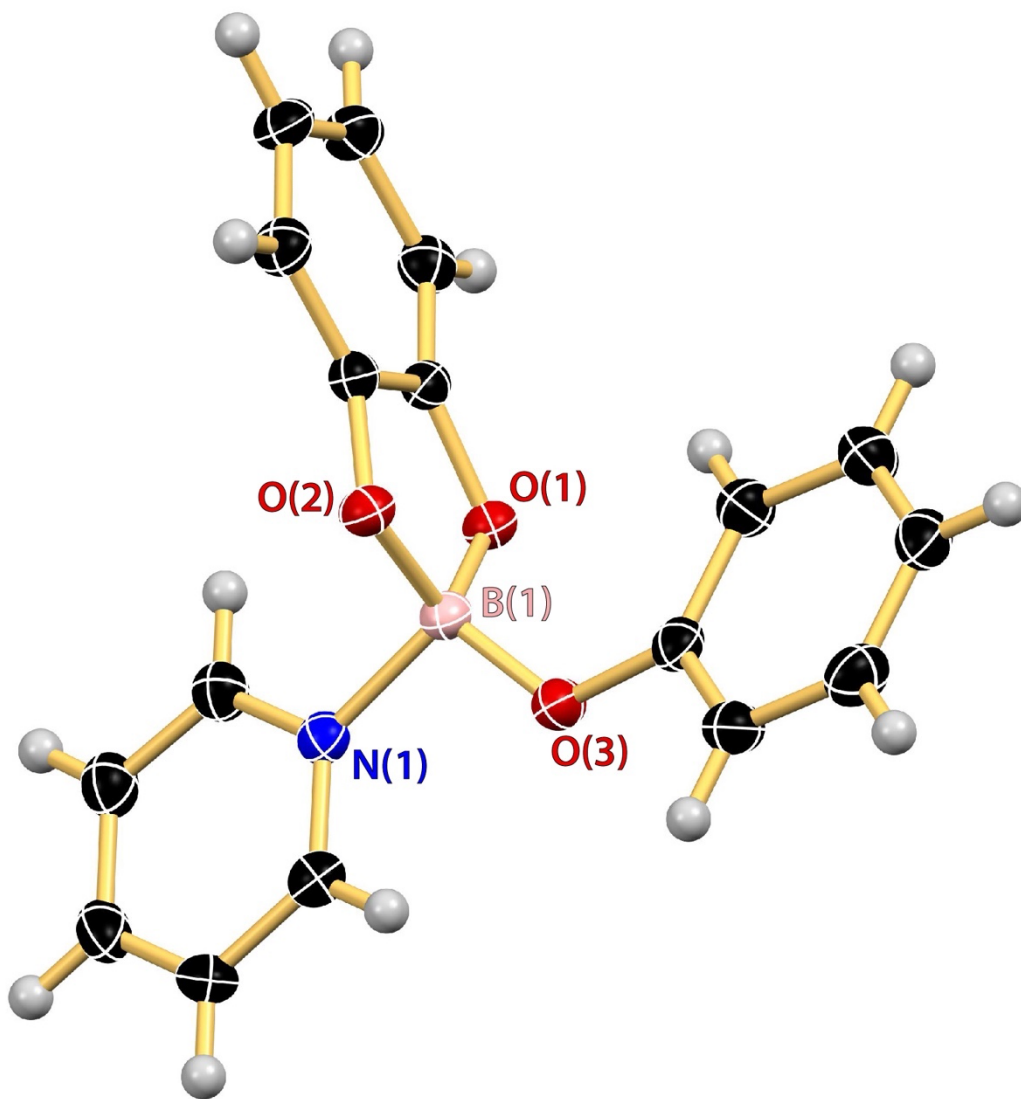


Figure S16. Thermal ellipsoid drawing (50%) of the solid-state structure of PhO(py)Bcat isolated from the synthesis of **3b**.

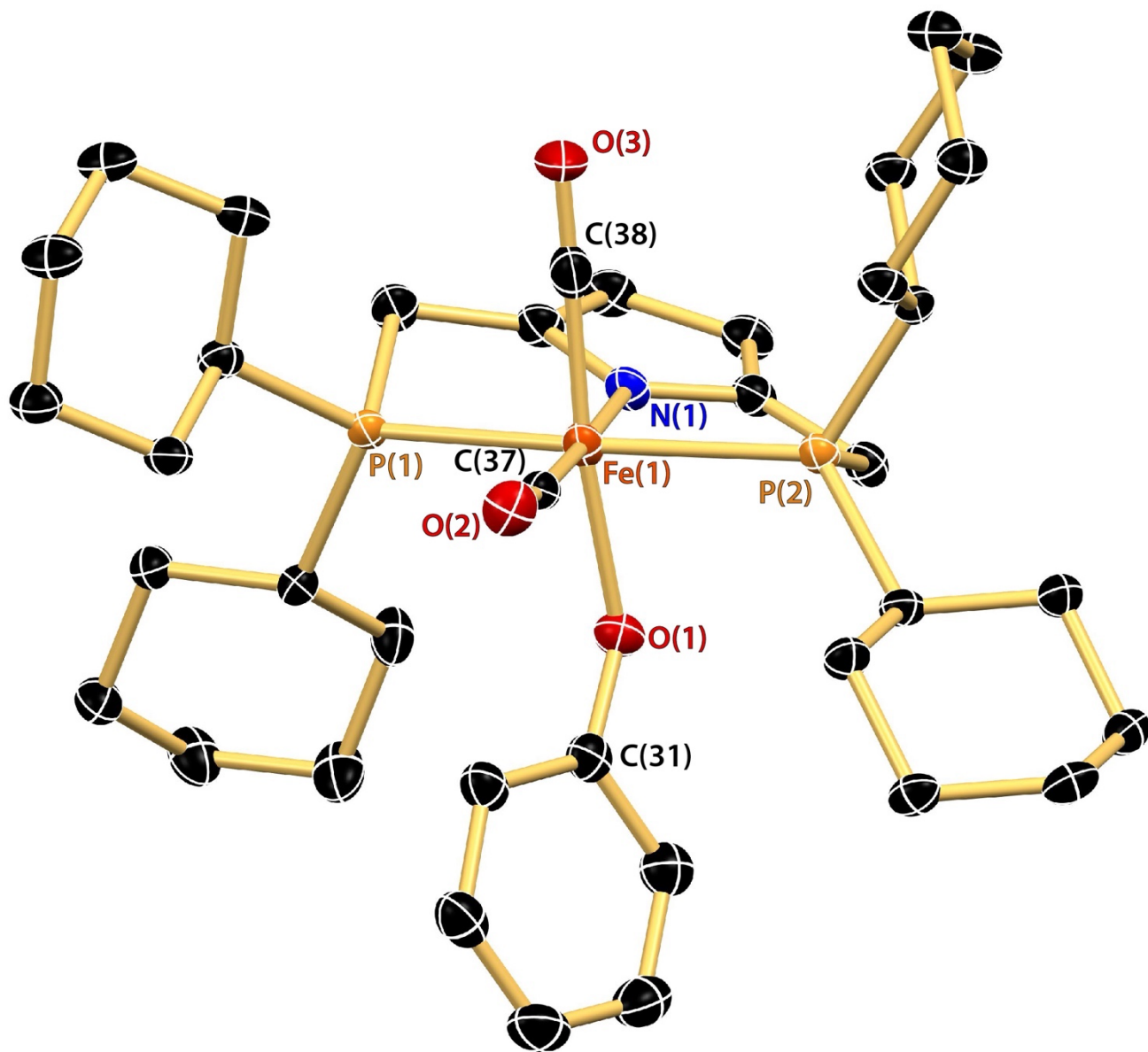


Figure S17. Thermal ellipsoid drawing (50%) of the solid-state structures of **1·CO**. Hydrogen atoms are omitted for clarity.

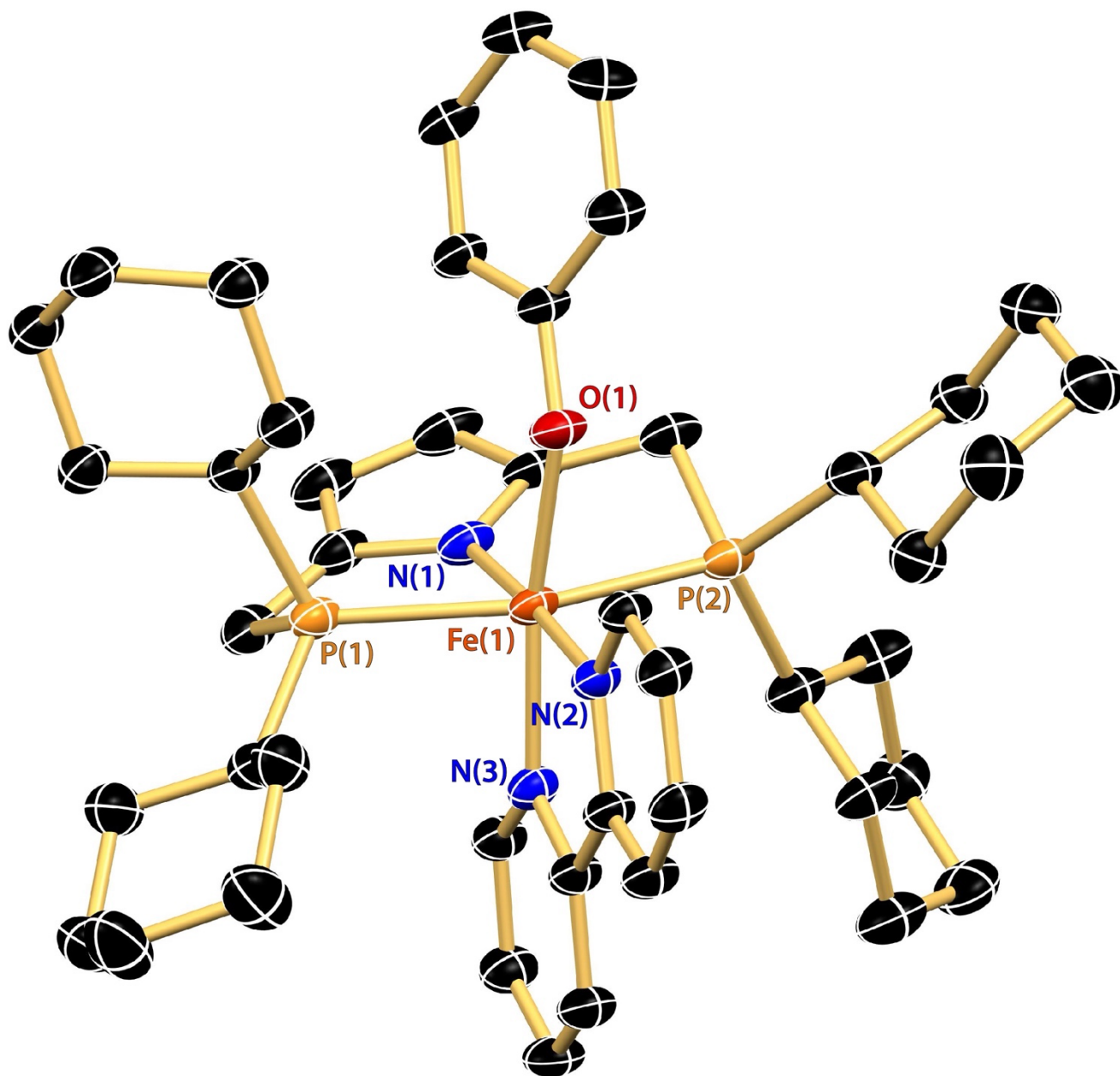


Figure S18. Thermal ellipsoid drawing (50%) of the solid-state structures of **1·bipy**. Hydrogen atoms are omitted for clarity.

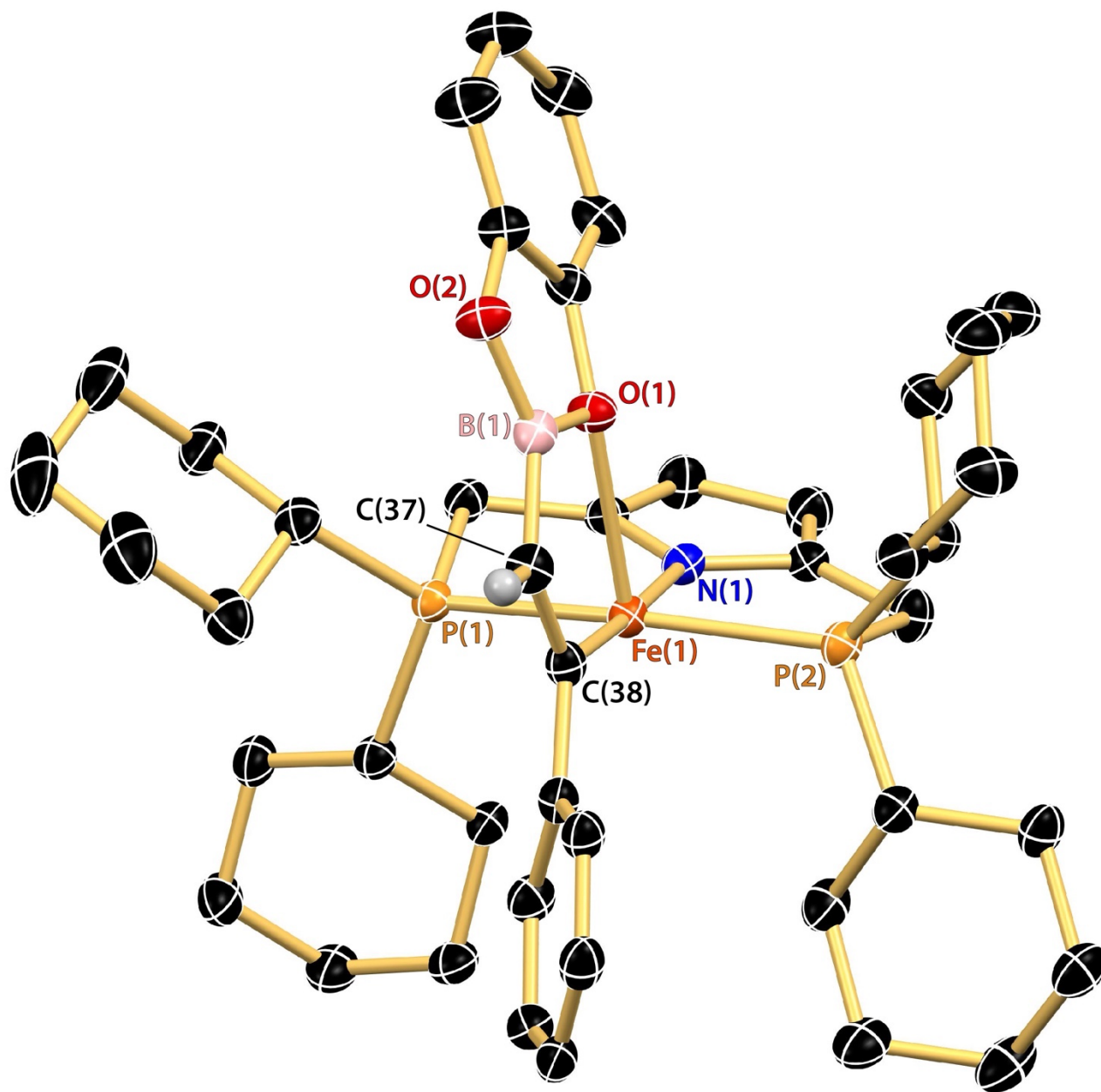


Figure S19. Thermal ellipsoid drawing (50%) of the solid-state structures of **5b**. Hydrogen atoms with the exception of that bound to C(37) are omitted for clarity.

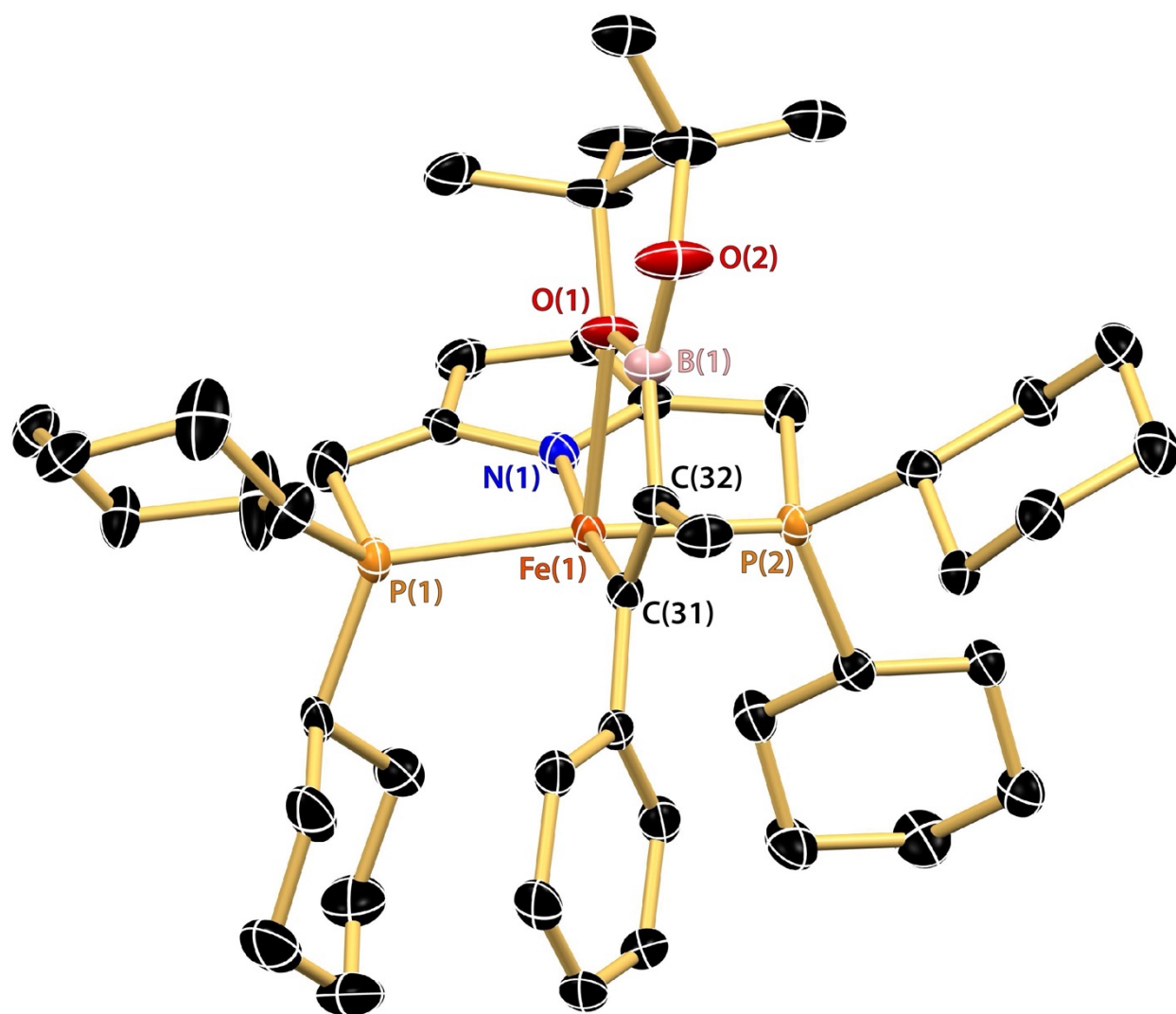


Figure S20. Thermal ellipsoid drawing (50%) of the solid-state structures of **6a**. Hydrogen atoms and minor components of the disorder are omitted for clarity.

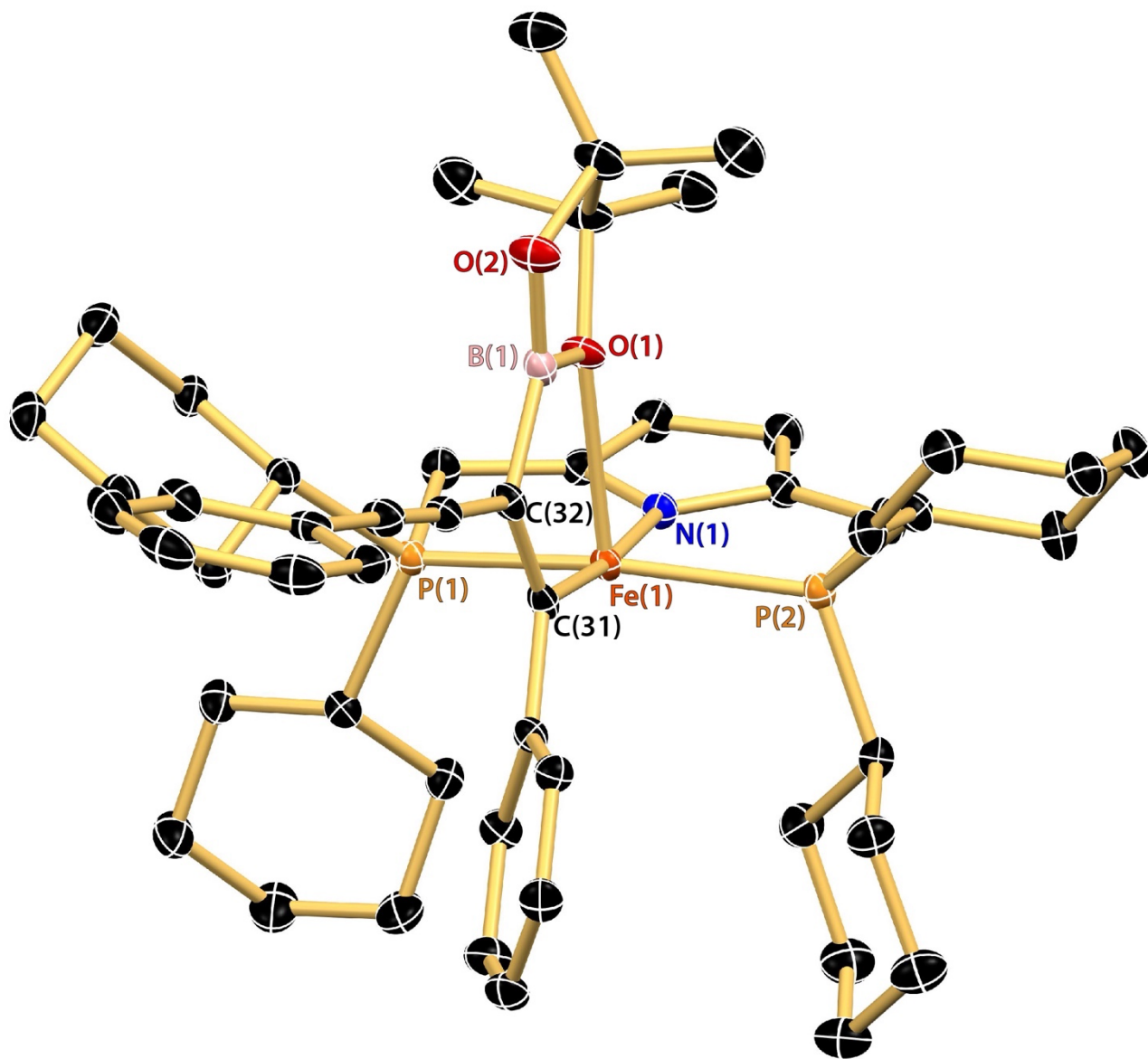


Figure S21. Thermal ellipsoid drawing (50%) of the solid-state structures of **7a**. Hydrogen atoms are omitted for clarity.